Supporting Information

Cobalt-Niobium Co-doping of Indium Oxide: Structural and Adsorption/Catalytic Properties for CO_2 Valorization

*Luis José Jiménez-Chavarriga,[a] Rocío Sayago-Carro,[a] Uriel Caudillo-Flores,[b] Irene Barba-Nieto,[c] Álvaro Tolosana-Moranchel,[a] José A. Rodriguez,[c,d] Marcos Fernández-García,[*a] and Anna Kubacka[*a]*

a) *Instituto de Catálisis y Petroleoquímica, CSIC. C/Marie Curie 2, 28049-Madrid, Spain.*
b) *Centro de Nanociencias y Nanotecnología, Universidad Nacional Autónoma de México, Ensenada 22800, México.*
c) *National Synchrotron Light Source II, Brookhaven National Laboratory, Upton 11973, NY, USA.*

Department of Chemistry, Stony Brook University, Stony Brook, NY, 11794, USA.

Email: mfg@icp.csic.es; ak@icp.csic.es

Catalytic set-up and details

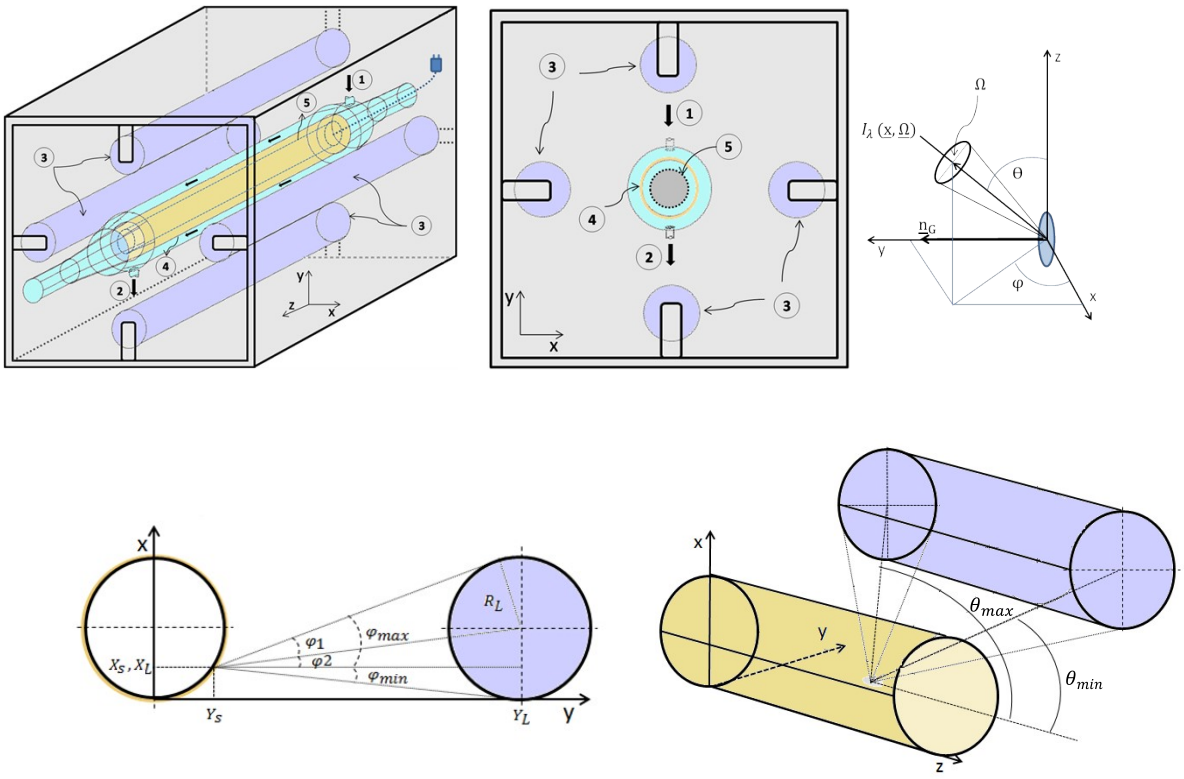

Figure S1. Upper, Left and Center: Photocatalytic annular reactor scheme; side and front views: (1) Gas inlet, (2) gas outlet, (3) UV lamp, (4) catalyst (brown) sample, (5) cartridge heater. q_{sup} Radiation flow on the surface of the sample (red), q_n radiation flow from the lamps (blue). Upper, Right: Center of coordinates located at the sample (defined by coordinates x_s, y_s, z_s). Down, Coordinate system to define the integration limits of the radiation Model. (Left) φ_{min} and φ_{max}. (Right) Θ_{min} and Θ_{max}.

The photo-thermal activity of the samples for methanol reforming was tested using a gas-phase continuous flow annular photothermal reactor (pyrex), schematically depicted in Figure S1. The catalyst (ca. 0.2 mg cm^{-2}) was deposited onto the inner tube (ca. 15 cm; 0.8 cm diameter) as a thin layer from a suspension in ethanol. A continuous rotation of the inner glass tube during

deposition and a careful evaporation procedure ensure the homogeneity of the (film) thickness obtained (see ref. 1 and references therein). During thermo-catalytic and photo-thermal-catalytic tests, the film was heated using a cartridge heater. The temperature of the layer was controlled and monitored by a temperature controller (Toho TTM-005) and a K-type thermocouple inserted into the reactor. Minimal (below 1 °C) axial temperature variation was reached with a cartridge heater (230 V; 500 W; "Resistencias RSI INCOLOID800") having controlled/compensated homogeneous heating. The UV irradiation was generated by four fluorescent UV lamps (Philips TL 6 W/08-F6T5 BLB, 6 W) symmetrically positioned outside the reactor. The lamps provide ca. 8 mW cm^{-2} intensity at the sample surface. The switching of the lamps only produces a modest change in temperature of less than 4 °C. Full details about energy distribution and illumination intensity can be obtained from previous publications [1]. The reacting mixture used a CO_2:H_2 1:1 ratio in a nitrogen carrier (2/2/6 mL min^{-1}).

The catalytic properties were evaluated from the start of the dark or irradiation period at fixed temperatures. The concentrations of the reaction products were analyzed using an online gas chromatograph (Agilent GC 8890) equipped with MolSieve-5A / HP-PLOT-Q/HP-Innowax columns (0.53/0.53/0.32 mm I.D. × 30 m) as well as thermal conductivity and flame ionization detectors. Catalytic tests were repeated 3 to 4 times and standard error values were calculated from the corresponding set of data.

In this work, catalytic output was measured with the help of three observables, the reaction rate, the quantum efficiency and the excess function of the reaction. The reaction rate (r) measures the number of CO_2 molecules per mass and time unit, but to analyze the photothermal valorization of CO_2 an "excess rate" (r_e) was measured through Equation S1.

$$r_e\,(\%) = 100 \times \left(r_{(\text{Photo-thermal})} - \left(r_{(\text{Photo})} + r_{(\text{Thermo})}\right) / \left(r_{(\text{Photo-thermal})}\right)\right) \quad \text{(S1)}$$

Such "excess" rate is expressed as a percentage in equation S1 and measures the potential synergy occurring between both energy sources in the photothermal catalytic process. Synergy is thus measured as the excess (i.e. positive value) over the additive effect of light (measured at room temperature, RT) and heat (150, 250, 350 °C) in the reaction rate.

The second is the Quantum Efficiency (QE) parameter valorization of CO_2. QE is defined by the IUPAC through Equation S2 [2].

$$QE(\%) = 100 \times \frac{r\ (mol\ m^{-2} s^{-1})}{e^{a,s}\ (Einstein\ m^{-2} s^{-1})} \quad \text{(S2)}$$

In this equation, r is the reaction rate and $e^{a,s}$ the average local superficial rate of photon absorption.

The rate of CO_2 elimination is measured by gas chromatography as previously outlined and normalized using the BET surface area of the sample. The local superficial rate of photon absorption ($e^{a,s}$) is defined by Equation S3. It follows from the equation corresponding to a pure photo-catalytic process, but with an additional term that accounts for the losses coming from charge emission with temperature [3]. In this equation, F_{As} is the fraction of light absorbed by the sample, q_{sup} the radiation flux at each position ($\underline{x} \equiv X_s, Y_s, Z_s$) of the catalytic film, and T_e is the thermal emission loss terminus.

$$e^{a,s}(\underline{x}) = \left(q_{sup}(\underline{x}) - T_e\right) F_{As} \quad \text{(S3)}$$

To obtain the radiation flow on the surface of the samples, first, it was calculated the impinging radiation flux from the lamps (q_n). Considering the coordinate system presented in Figure S1 and the geometry of the reactor (annular multi-lamp), the q_n can be determined by Equation S4 [1].

$$q_n\left(X_s,Y_s,Z_s\right) = \sum_{L=1}^{L=4}\sum_{\lambda}\int_{\varphi_{min,L(x,y)}}^{\varphi_{\max,L(x,y)}}\int_{\Theta_{min(x,y,\varphi)}}^{\Theta_{max(x,y,\varphi)}} \frac{P_{\lambda,L}}{2\pi\, R_L\, Z_L}\, sin^2\Theta \left(\left(\frac{X_s - X_L}{R}\right)\cos\varphi + \left(\frac{y_s}{R}\right) sin\varphi\right) d\varphi d\Theta \quad \text{(S4)}$$

Where Xs, Ys, Zs are the coordinates of the points located on the surface of the catalytic film, and X_L, Y_L, Z_L which are the coordinates of the points located on the surface of the lamp. R type variables correspond to the radius of the cylinder supporting the sample (R) or of the lamp (R_L), see Figure S1. Angular variables (Θ,φ) are defined as described in Figure S1. A detailed description of the mathematical formulation to provide q_{sup} as a function of q_n and the transmittance/reflectance optical measurements for each component of our reactor system can be found elsewhere [1,4].

The T_e is a loss term and can be calculated using Equation S5. This Equation considers the emission of a body in a medium can be calculated using Plank´s law [3]. The radiation intensity per surface area unit is [3,5]:

$$T_e = \frac{n^2\pi\, h\, T^4}{c^2}\int_0^{\infty}\frac{\gamma^3\,\alpha(\gamma,T)}{e^{\frac{h\gamma}{k\,T}} - 1}\, d\gamma \quad \text{(S5)}$$

Where γ is the photon frequency, h is the Plank´s constant, c is the speed of light, n is the refraction index of the solid, k is the Boltzmann´s constant, T is the temperature of the sample and α is the absorption efficiency that acts as an emissivity type factor as discussed in refs. 4,5.

Catalytic and Characterization Results

Table S1. ICP-OES results for Co and Nb molar content of the solids.

Sample	Co / %	Nb / %
In4Co	4.2	-
In5Nb	-	5.2
In4Co2.5Fe	4.2	2.6
In4Co5Nb	4.1	5.3
In4Co7.5Nb	4.2	7.8_5

Table S2. Photothermal reaction rate, excess rate, and selectivity to CO at 250 °C as a function of the H_2:CO_2 ratio of the feed (10 mL min^{-1}) for the In4Co5Nb.

Parameter	H_2:CO_2 ratio		
	1:1	2:1	3:1
Rate (mmol g^{-1} h^{-1})	2.98	2.54	2,07
Excess (%)	49.0	58.0	41.0
Selectivity (%)	99.7	99.4	99.2

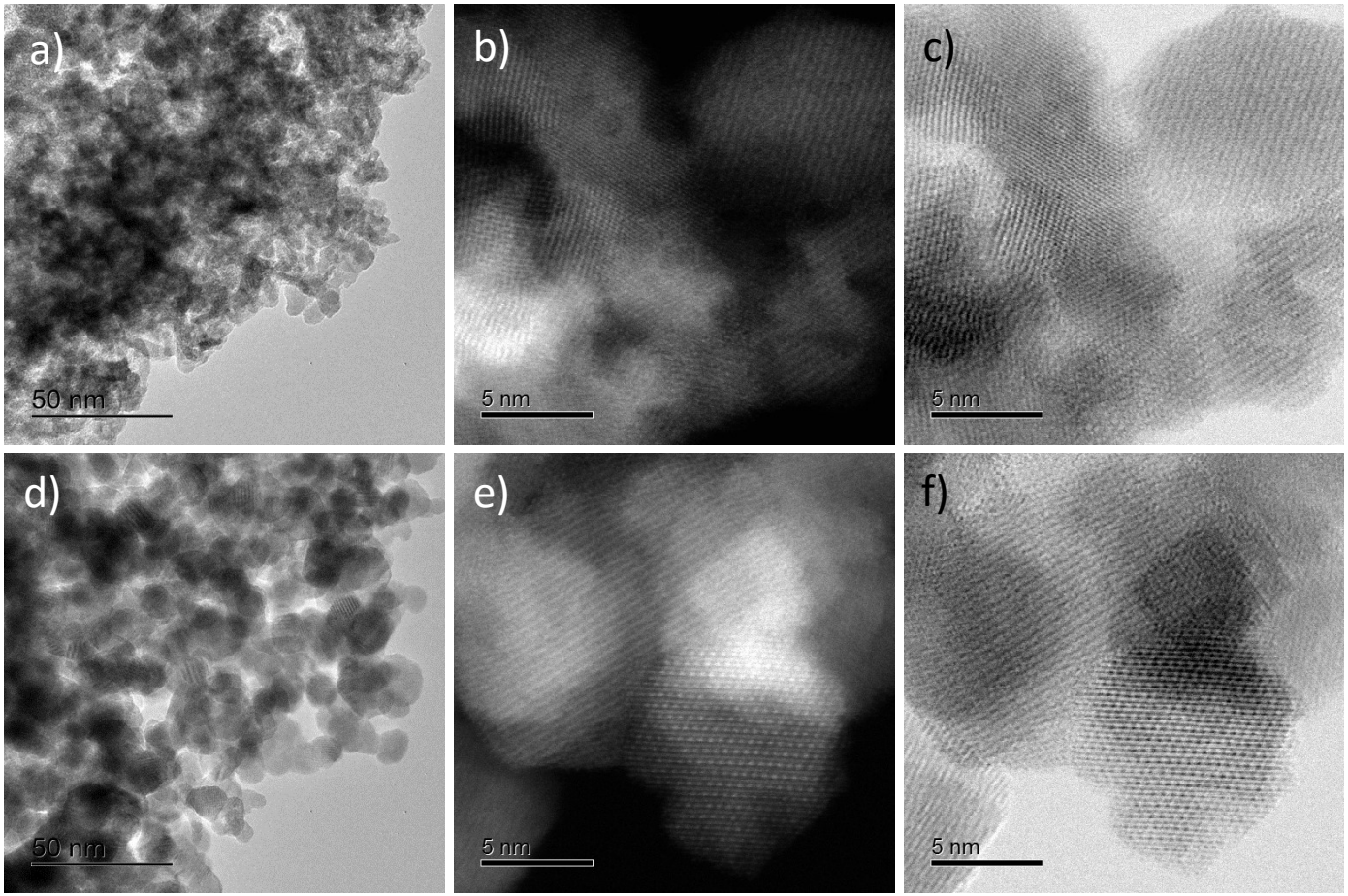

Figure S2. Bright and dark-field HR-TEM images of the In4Co2.5Nb (a-c) and In4Co7.5Nb (d-e) samples.

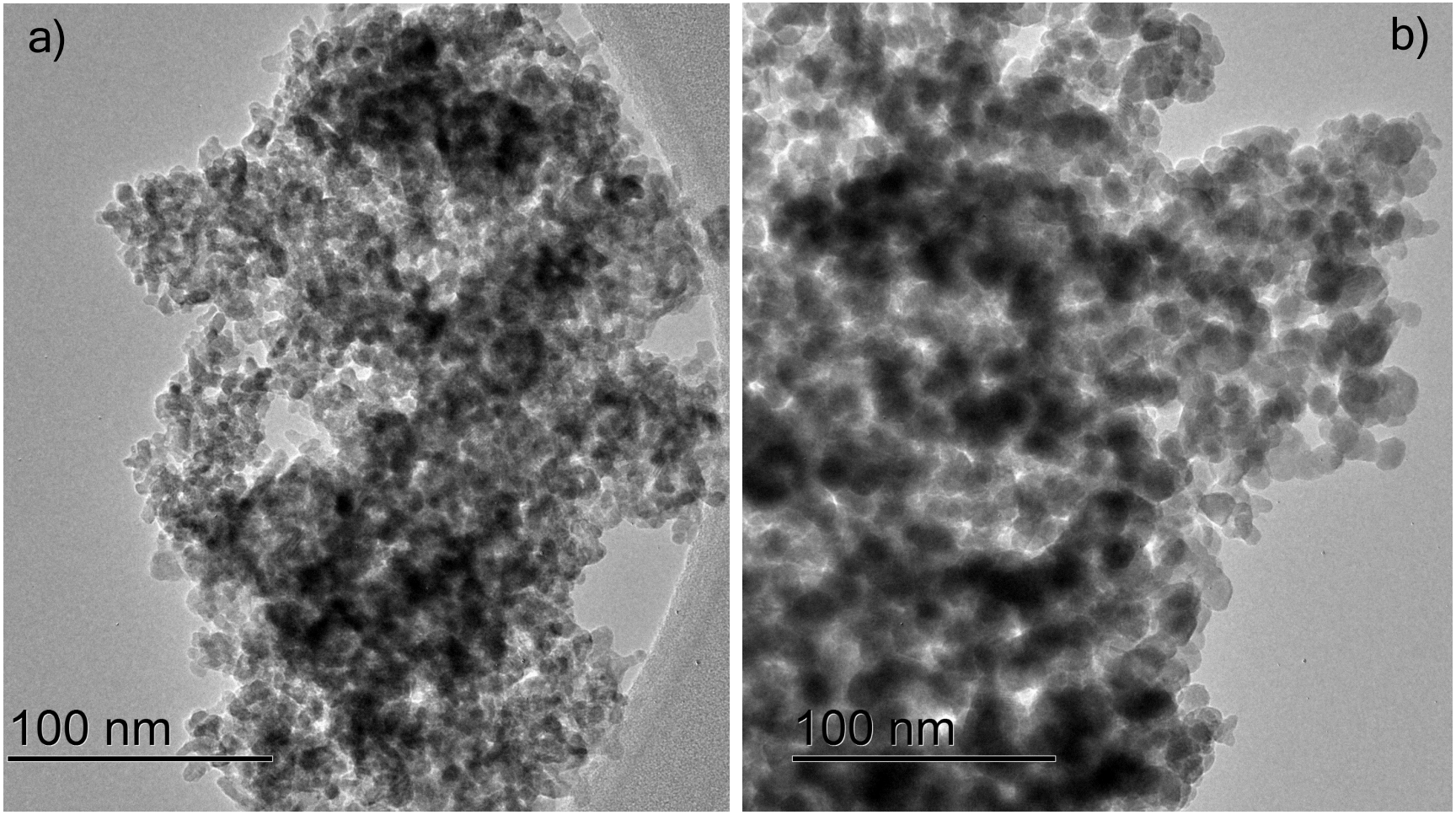

Figure S3. TEM images showing the change from the batonnet-type (a; In4Co) to the rounded-type (b; In4Co7.5Nb) shape of the primary particle size through the samples.

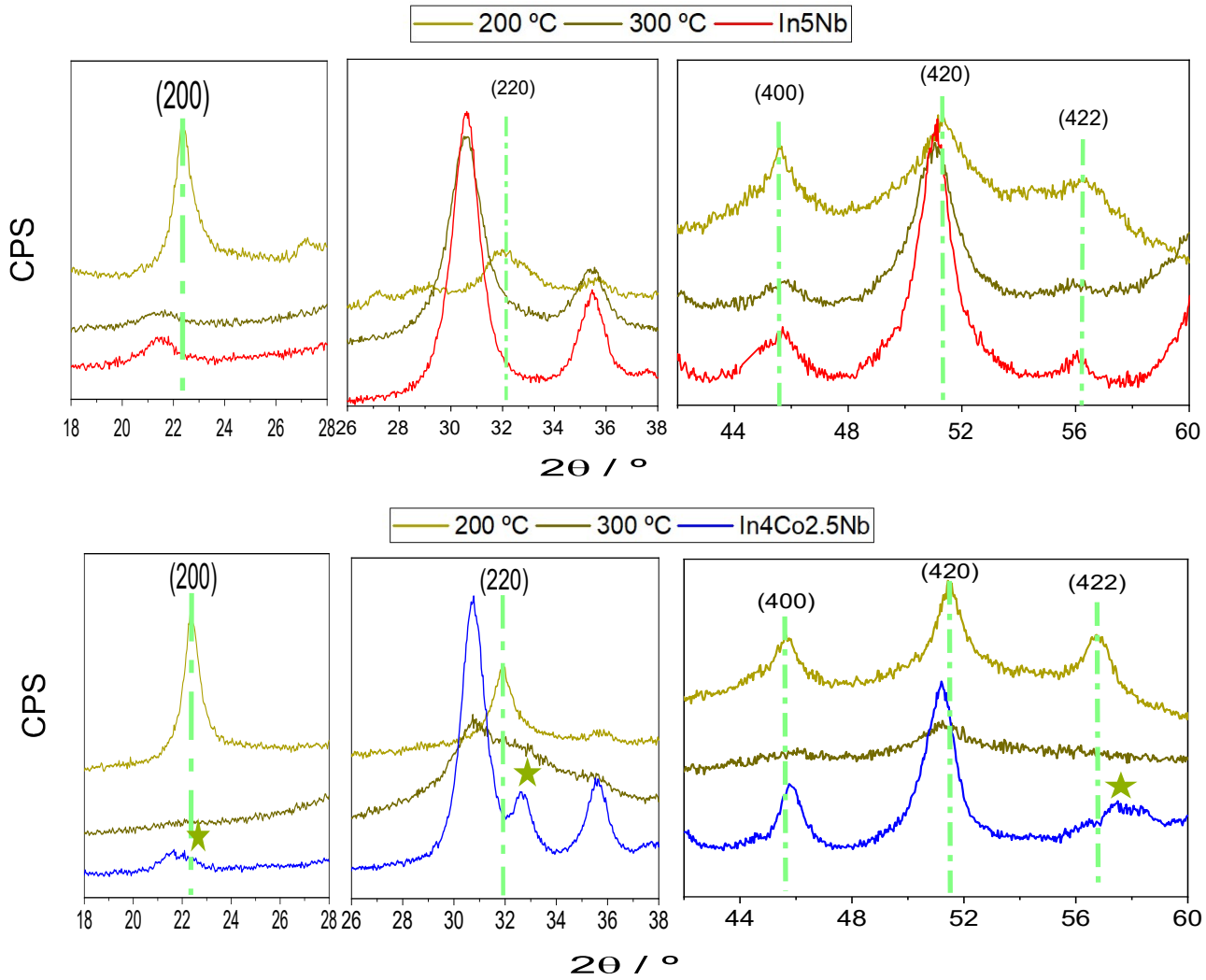

Figure S4. XRD patterns obtained under a calcination ramp for the In5Nb and In4Co2.5Nb samples.

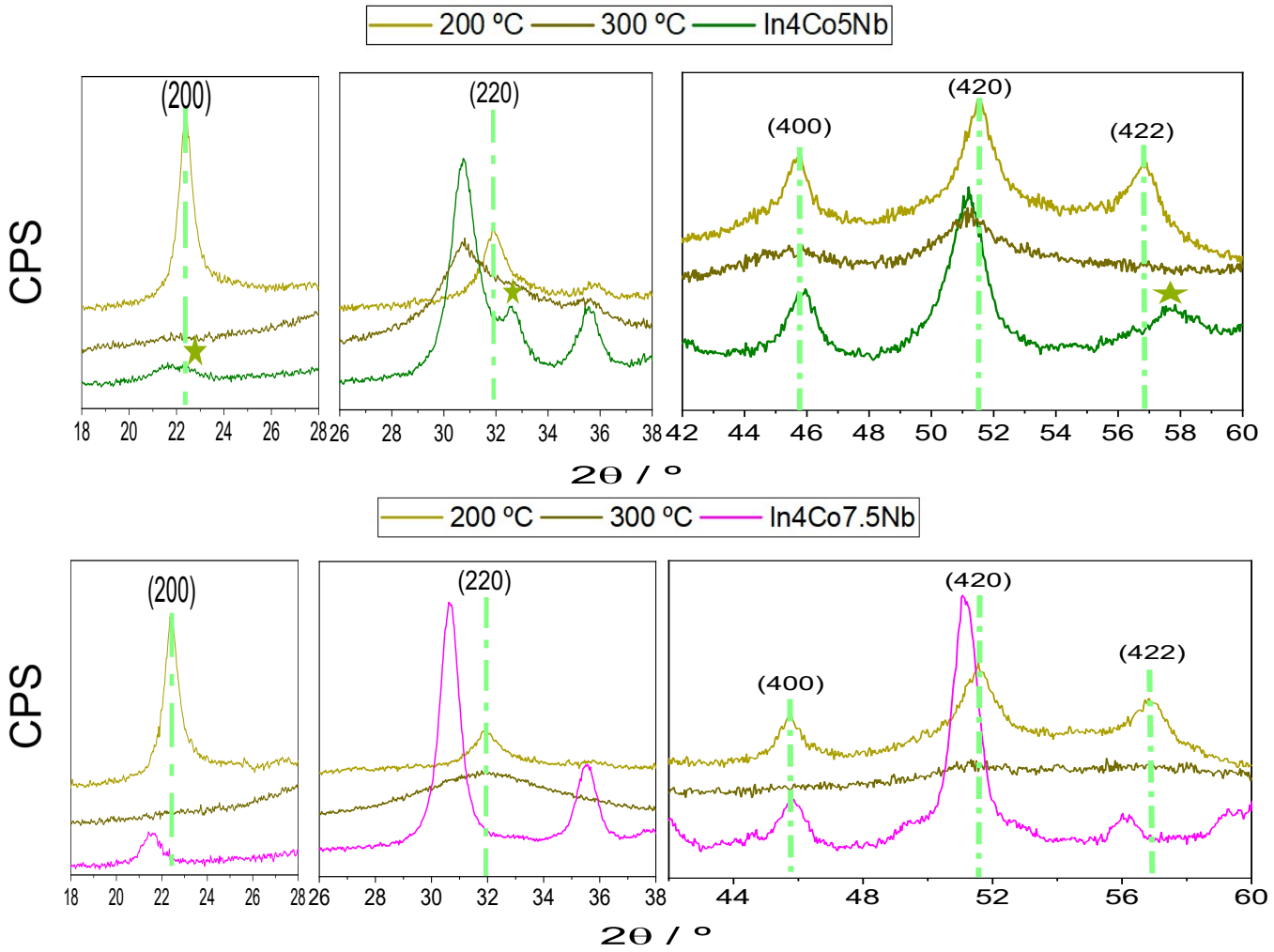

Figure S5. XRD patterns obtained under a calcination ramp for the In4Co5Nb and In4Co7.5Nb samples.

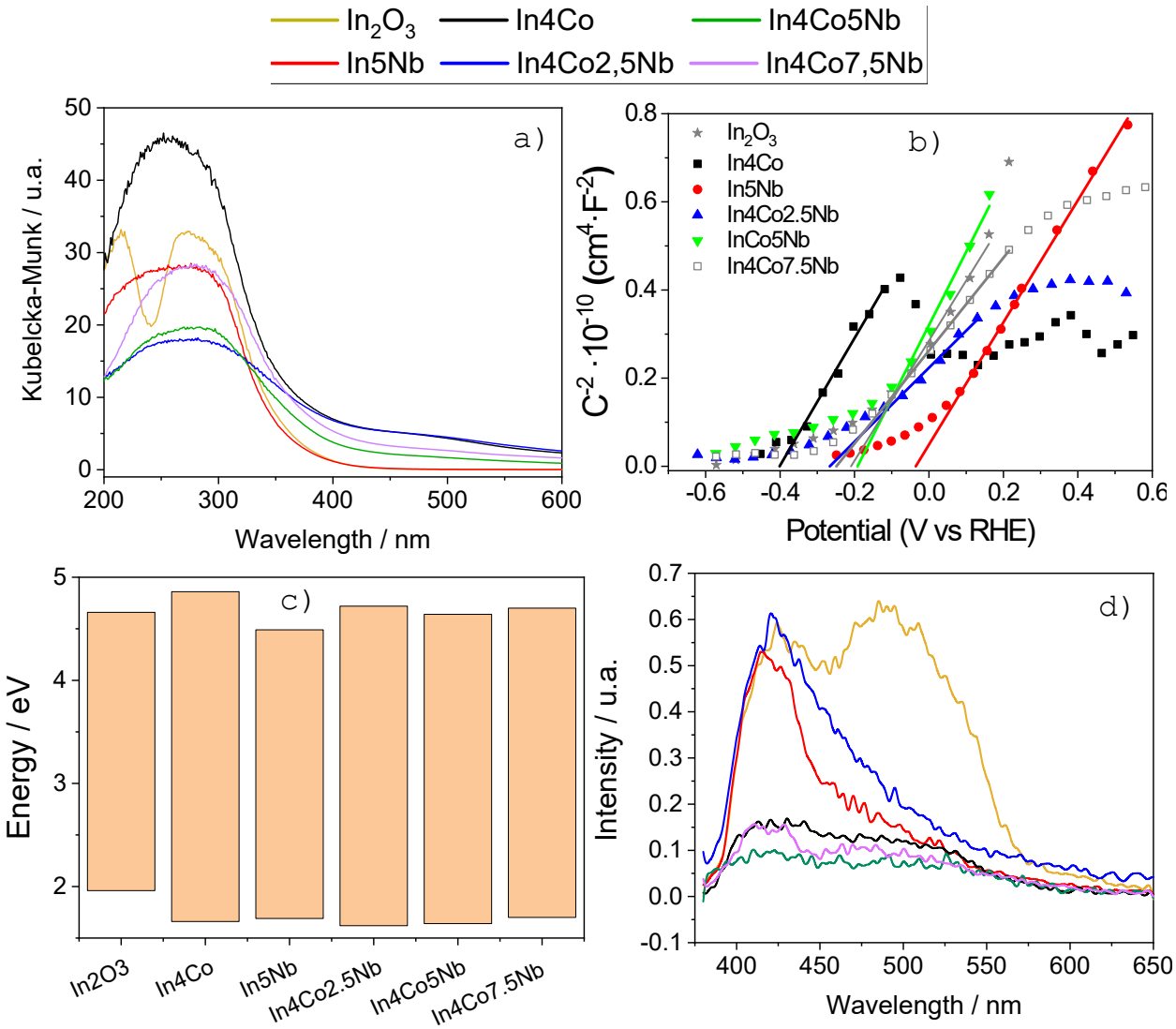

Figure S6. (a) UV-visible spectra for the samples; (d) Mott-Schottky plot for the samples; (c) Valence and conduction band-edge and band gap energy (absolute energy scale) for the samples; and (d) Photoluminescence spectra (λ_{exc} 365 nm) for the samples.

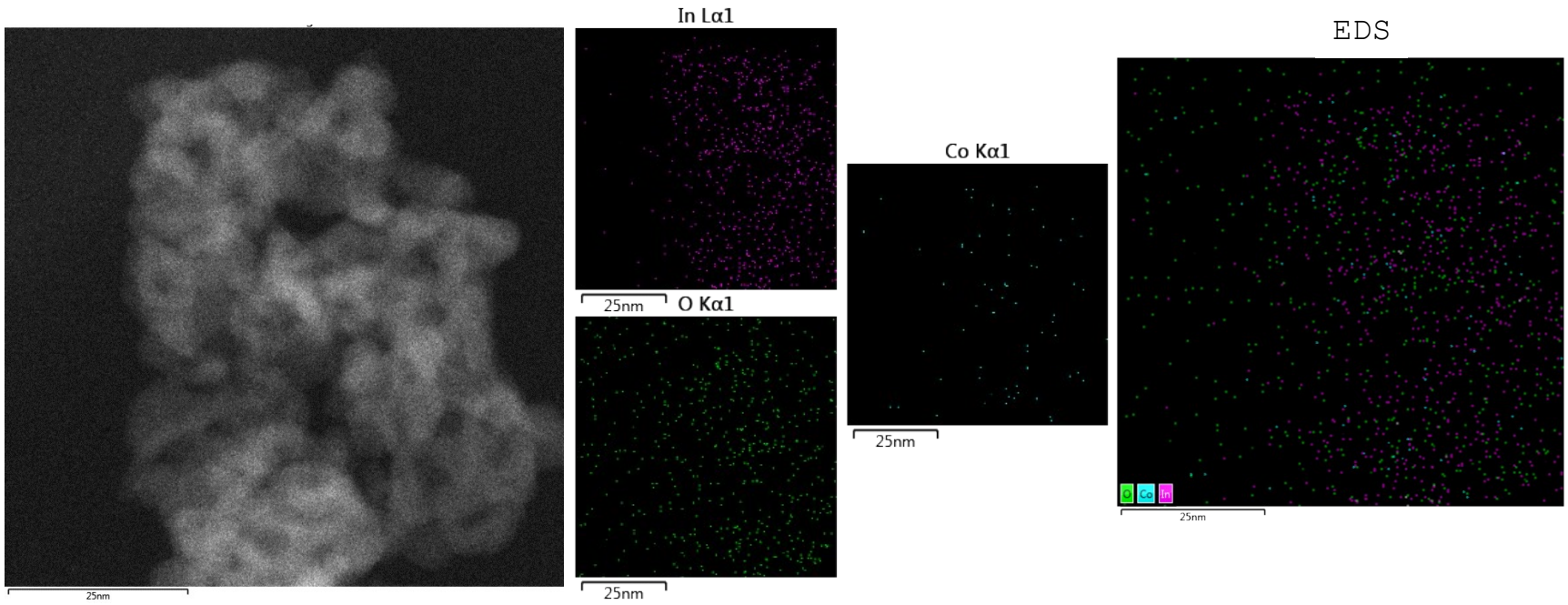

Figure S7. Dark-field RH-TEM micrograph and EDS analysis of the In4Co sample.

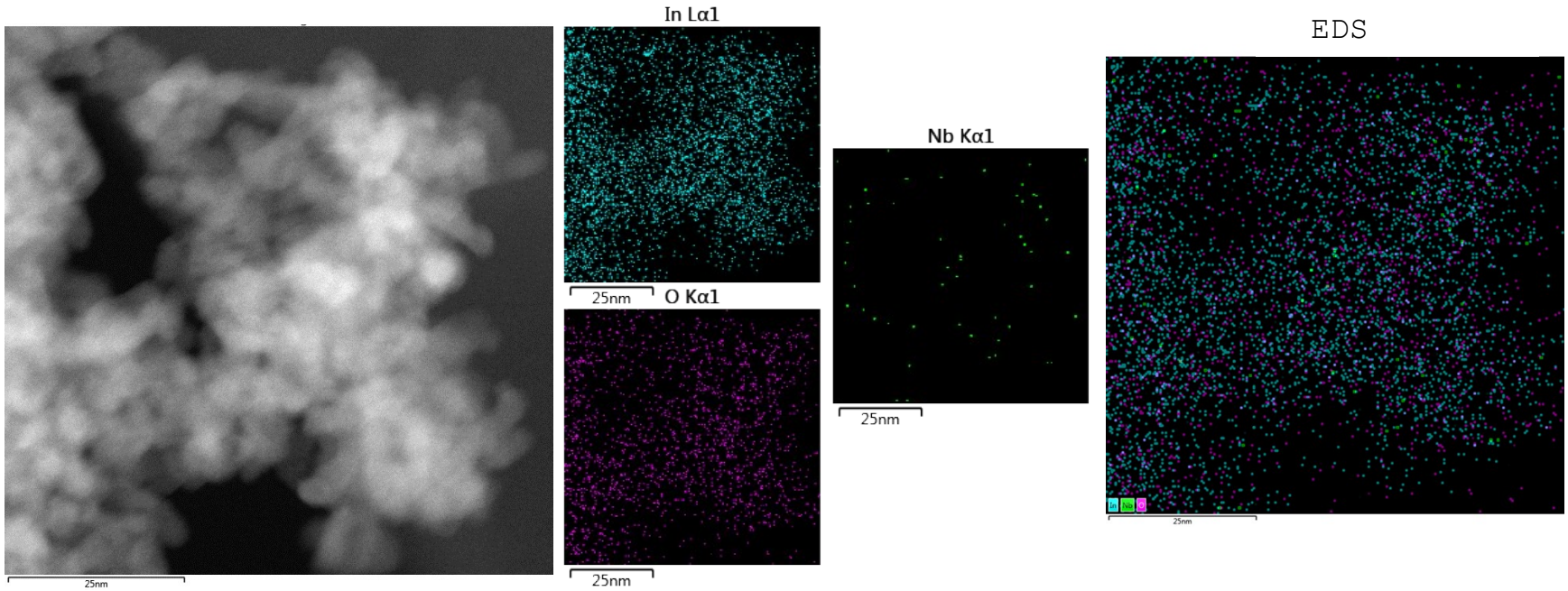

Figure S8. Dark-field RH-TEM micrograph and EDS analysis of the In5Nb sample.

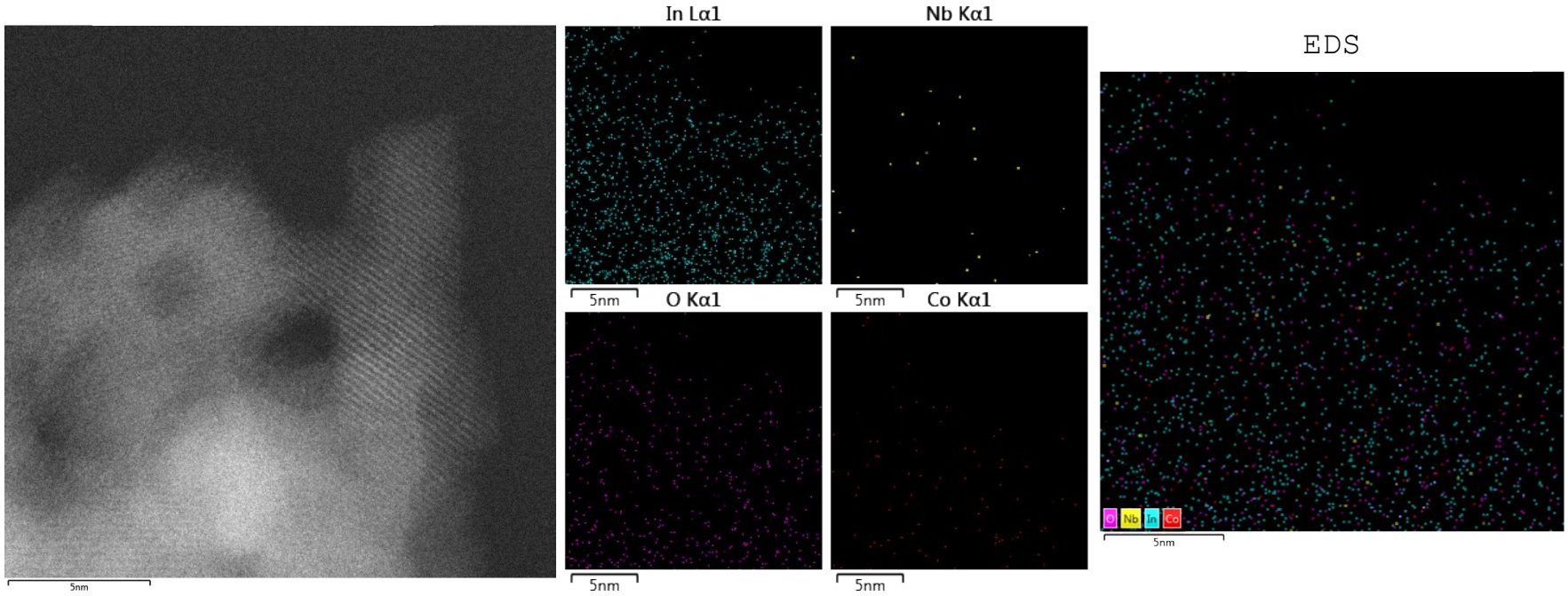

Figure S9. Dark-field RH-TEM micrograph and EDS analysis of the In4Co5Nb sample.

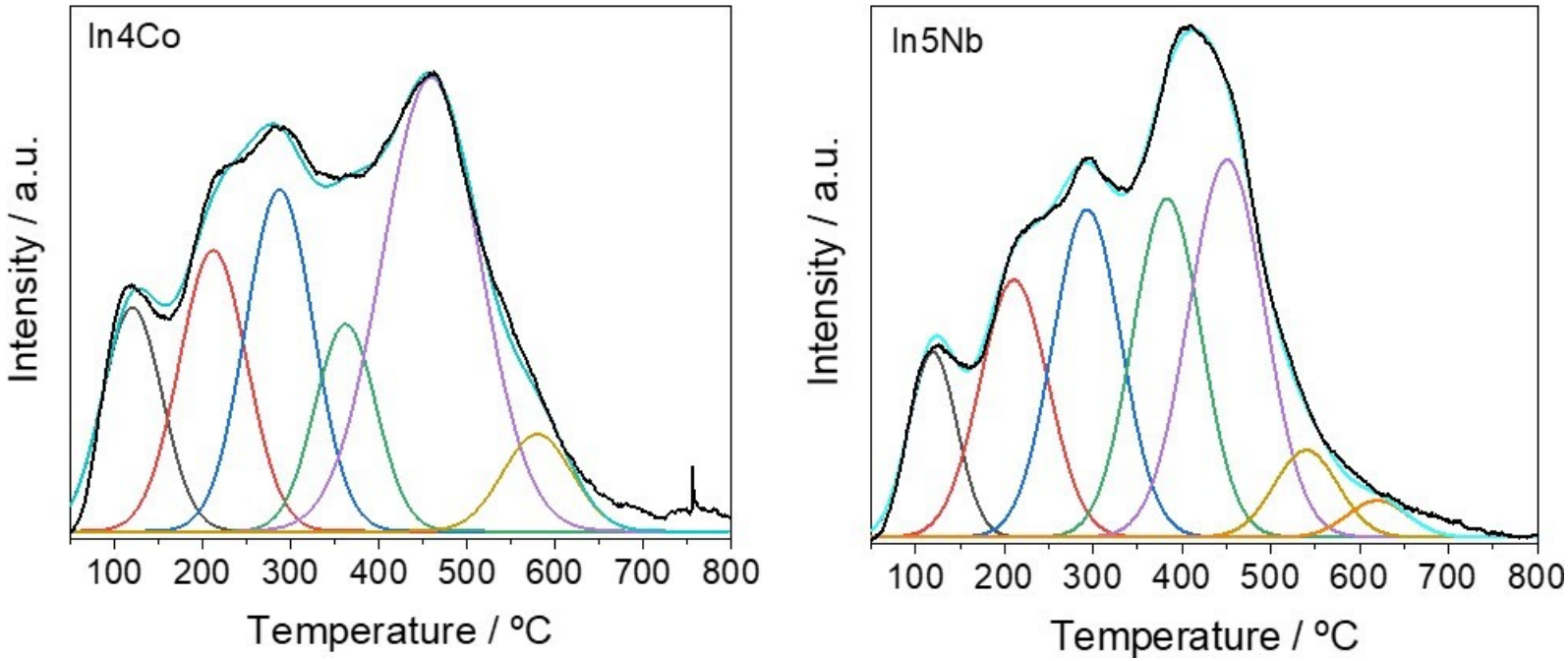

Figure S10. TPD results for reference samples.

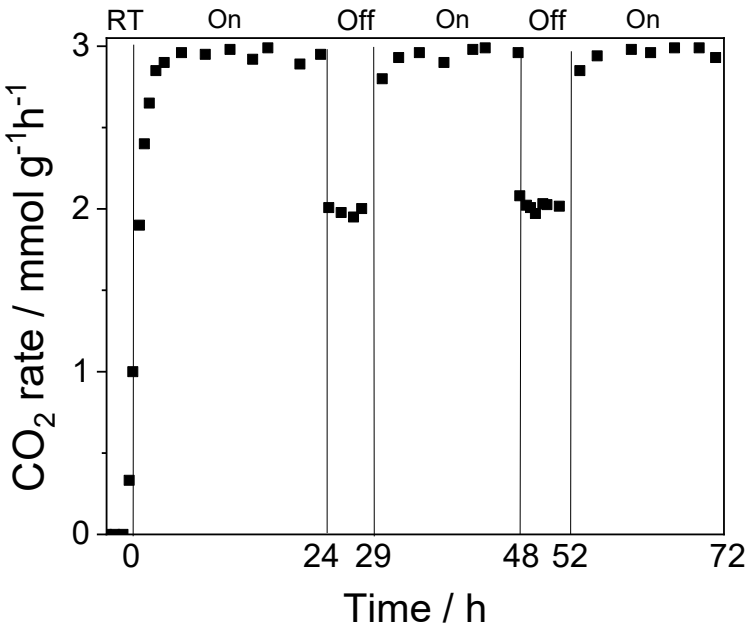

Figure S11. Reaction rate as a function of time during a three on-off (thermo-photothermo) cycling test at 250 ℃ using the In4Co5Nb sample.

References

1 M.J. Muñoz-Batista, A. Kubacka, A.B. Hungría, M. Fernández-García. Heterogeneous photocatalysis: Light-matter interaction and chemical effects in quantum efficiency calculations. J. Catal. 330 (2015) 154–166.

2 S.E. Braslavsky, A.M. Braun, A.E. Cassano, A.V. Emeline, M.I. Litter, L. Palmisano, V.N. Parmon, N. Serpone. Glossary of terms used in photocatalysis and radiation catalysis (IUPAC Recommendations 2011). Pure Appl. Chem. 83 (2011) 931-1014. http://dx.doi.org/10.1351/PAC-REC-09-09-36

3 G.W. Kattawar, M. Eisner, Radiation from a homogeneous isothermal sphere. Appl. Optics 9 (1970) 2685-90.

4 G.E. Imoberdorf, H.A. Irazoqui, A.E. Cassano, O.M. Alfano. Photocatalytic Degradation of Tetrachloroethylene in Gas Phase on TiO2 Films: A Kinetic Study. Ind. Eng. Chem. Res. 44 (2005) 6075–6085. https://doi.org/10.1021/ie049185z

5 C.F. Bohm, D.R. Hoffman, Absorption and scattering of light by small particles. Whiley (1999) New York.